DTU Library

Aging of 3D-printed maraging steel

Thorsteinsdóttir, E. G.; Primdahl, D. S.; Zhang, Y. B.; Juul Jensen, D.; Yu, T.

Published in:
I O P Conference Series: Materials Science and Engineering

Link to article, DOI:
10.1088/1757-899x/580/1/012047

Publication date:
2019

Document Version
Publisher's PDF, also known as Version of record

IOP Conference Series: Materials Science and Engineering

Aging of 3D-printed maraging steel

IOP Conf. Series: Materials Science and Engineering **580** (2019) 012047 doi:10.1088/1757-899X/580/1/012047

Aging of 3D-printed maraging steel

E G Thorsteinsdóttir[1], D S Primdahl[2], Y B Zhang[1], D Juul Jensen[1] and T Yu[1]

[1] Department of Mechanical Engineering, Technical University of Denmark, DK-2800 Kgs. Lyngby, Denmark
[2] Grundfos A/S, DK-8850 Bjerringbro, Denmark

tiyu@mek.dtu.dk

Abstract. The effects of aging on the microstructural development and mechanical properties of a 3D-printed maraging steel have been investigated. The microstructures within printed, solution treated and aged samples are characterized by X-ray tomography and optical microscopy, as well as by scanning and transmission electron microscopy. The mechanical properties are estimated based on hardness measurements. The distribution of voids is found to be inhomogeneous, and even though the samples are 99.9% dense in the sample interior, the remaining voids affect significantly the hardness in the aged condition. In addition to precipitation, the aging treatment leads to formation of about 12% of reverted austenite. Together this leads to a strengthening of the material. Solution treatment results in homogenization of the microstructures such that after aging the solution treated samples are found to have higher strength than the samples that are just aged after printing. These results are discussed and compared to the aging behaviour of conventionally manufactured samples.

1. Introduction

Additive manufacturing in the form of 3D printing is a new popular manufacturing process, currently undergoing rapid growth [1]. Huge investments worldwide have been made, related to the development of new machines and processes, as well as to the production of suitable powders and education of users. The development of this technique has been fast, and today 3D printing is not only used for prototypes but also for manufacture of components. It is expected that 3D printing will be used even more extensively in the future, both to re-design current products and for new designs based on the possibilities in 3D printing.

One of the materials often used in 3D printing is maraging steel. This is a popular material because of its good weldability and superior mechanical properties, which make it ideal for tool manufacturing. Maraging steel is strengthened through aging, leading to precipitation of intermetallic particles [2]. Important parameters are the aging temperature and time, which are known to have a large influence on the mechanical properties [3].

In conventional manufacturing, maraging steels are typically solution treated [3], which is generally not the case for 3D-printed material. It is, therefore, not surprising that similar aging of 3D-printed and conventionally manufactured samples does not result in the same mechanical properties. An additional complication is that 3D-printed samples may contain fractions of retained austenite and reverted austenite after aging. It has been suggested that this austenite may contribute to the less good mechanical properties of 3D-printed samples compared to equivalent ones manufactured conventionally, where austenite reversion typically only occurs at higher temperatures [4,5].

The aim of the present work is to investigate the effects of aging on the microstructural development and the mechanical properties of 3D-printed maraging steel samples and to compare these effects with those for conventionally manufactured samples. Finally post-printing solution treatment is also considered, and effects of such treatments are discussed.

2. Experimental Details

The samples were printed by selective laser melting using a dual laser system (two 400 W lasers) according to standard industrial practice. Spherical shaped magaing steel powder with size range 10 - 45 µm was used for printing. In total 38 samples with size 3 × 6 × 12 mm^3 and 10 samples with size 22 × 200 × 5.3 mm^3 were printed. For comparison, a rod of maraging steel with a similar nominal chemical composition (table 1) was used.

Table 1. Chemical composition of the maraging steel rod (in wt.%).

Ni	Mo	Co	Ti	Cr	S	P	Mn	Si	C	Fe
17.0-19.0	4.5-5.2	8.5-10.0	0.8-1.2	≤0.25	≤0.01	≤0.01	≤0.15	≤0.1	≤0.03	Bal.

Aging was carried out at 480, 500, 520 and 540 °C for 1 to 10 h. For additional 3D-printed samples, a solution treatment at 850 °C for 1 h was also carried out before aging at 500 °C. All samples were air cooled.

The mechanical properties were quantified by Vickers hardness measurements using a load of 500 g for 10 s in the longitudinal section (containing the building direction). The reported hardness values are averaged over at least 6 measurements.

The microstructures in the longitudinal section were characterized by optical microscopy, scanning electron microscopy (SEM) and transmission electron microscopy (TEM). Additionally absorption contrast X-ray tomography was used to detect voids non-destructively in 3D. For optical microscopy and SEM observations, samples were mechanically polished followed by etching in a 2% Nital solution. For electron backscatter diffraction (EBSD) studies, samples were mechanically polished using OP-U colloidal silica suspension (40 nm particle size) for the final step. For the TEM observations, thin foils were prepared using a modified window technique.

The X-ray tomography characterization was performed using a Zeiss Xradia 520 Versa X-ray microscope. A detector (2032 × 2032 pixels) with pixel size of 3.36 µm was used for recording absorption patterns. For determination of the distribution of voids in 3D, a 3 × 3 × 6 mm^3 sample aged at 500 °C for 6 h was used. During the high-resolution X-ray measurements, only one quarter of the cross section was analysed, in the top part of the sample (ca. 1.5 × 1.5 × 1.5 mm^3), and the sample was rotated through 360° in 4051 steps. The resulting spatial resolution is estimated to be 2 µm (voxel size 1.556 µm). Avizo was employed to visualize the voids.

3. Results and discussion

The distribution of voids is shown in figure 1. The voids are primarily distributed in the sub-surface layers (50-150 µm from surface). In the outer zone the voids are many and relatively large (see zone 1 in figure 1b). Here the sample density is only 97.9% while in the 2 inner zones the density is 99.9%. That the outer surface is more porous is in agreement with general observations for 3D-printed samples and is related to the lack of subsequent re-melting for these outer layers. For the 2 inner zones it is worth noticing that the sizes (equivalent spherical radii) of the voids in zone 2 (see figure 1b) are large, up to 20 µm, while in zone 3 the sizes do not exceed 15 µm and most of the voids are below 5 µm.

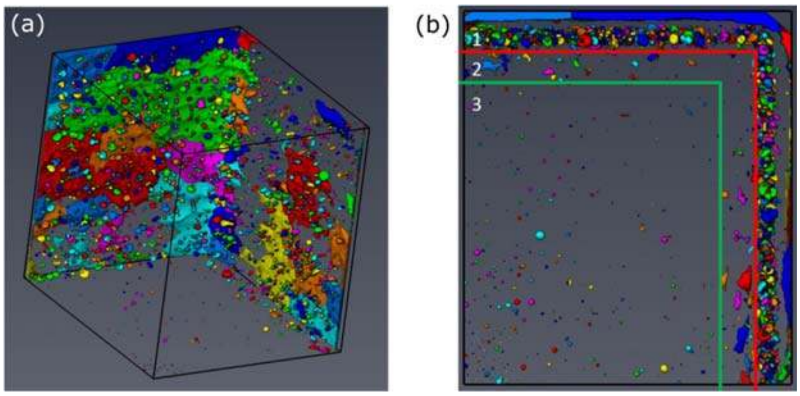

Figure 1. The distribution of voids inside a 3D-printed sample – only a quarter of the top part is shown (ca. 1.5 × 1.5 × 1.5 mm^3). The voids are shown in random colours, and some part of the surface is also coloured. a) Full 3D view, b) 2D projection, seen from the top.

The microstructures observed by optical microscopy are shown in figure 2. The meltpools are clearly visible in the as-printed and in the aged conditions, see figure 2a and b. In the samples that were solution treated before aging (see figure 2c) the microstructure is homogenized and the meltpools are no longer visible. However, in this condition a lath martensitic structure is visible, which is typical in maraging steels after conventional processing (including solution treatment and aging). This conventional martensitic structure is not observed if the sample is just aged without solution treatment after printing (see figure 2b).

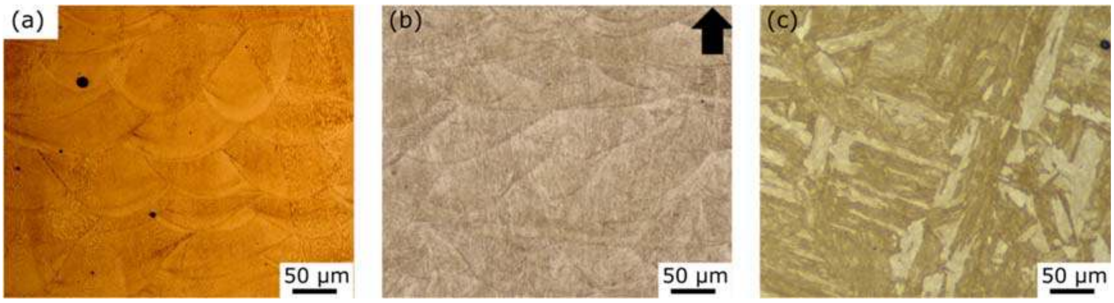

Figure 2. Optical micrographs of the printed and heat treated samples. a) in the as printed condition, b) aged at 480 °C for 1 h and c) solution treated at 850°C and aged at 480 °C for 6 h. The arrow indicates the common building direction.

Much more detail about the microstructure is revealed by SEM and TEM. High magnification investigations by SEM electron channelling contrast (ECC) imaging reveal the cell structure of the printed sample (figure 3a). Both equiaxed cells and elongated cell structures are observed. This is in agreement with literature results [4,6-8] and is consistent with EBSD characterization of the present sample, suggesting these cells are bounded by low angle dislocation boundaries formed during cooling. After aging, the structure is dominated by extended features which by EBSD are revealed to be austenite (see figures 3c and 4). After solution treatment, the printing-induced cells are no longer observed, and instead the typical martensitic structure is clearly visible (figure 3b). Aging of this sample results in precipitation (see figure 3d), as in conventionally manufactured maraging steel samples. No austenite is apparent in the solution treated and aged samples.

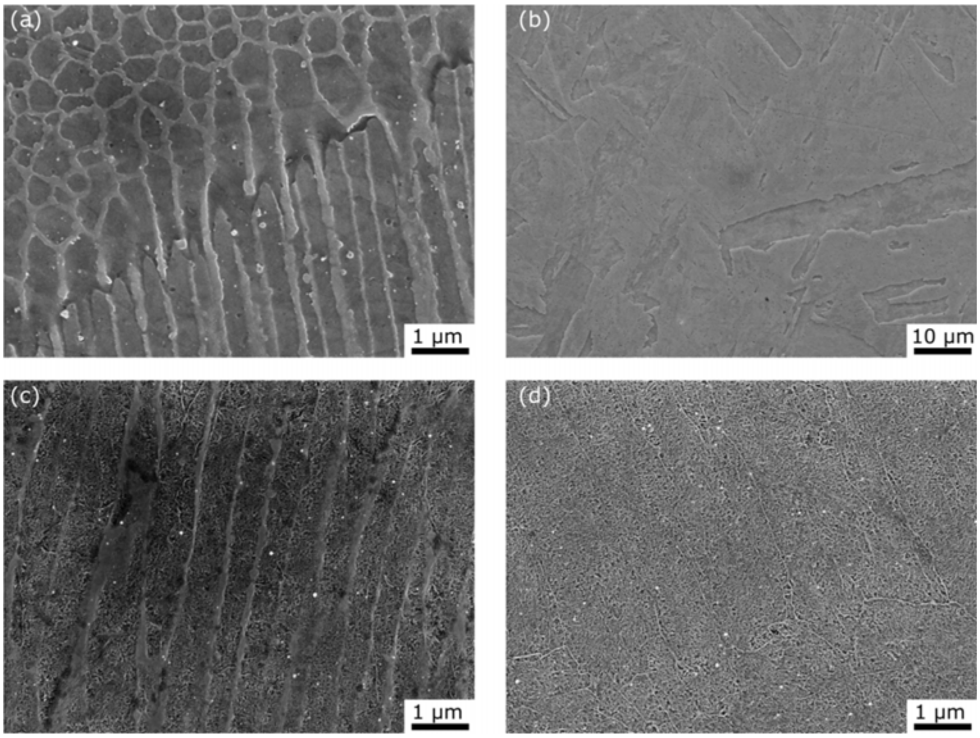

Figure 3. SEM micrographs of printed and heat treated samples. a) the as-printed condition, b) solution treated at 850 °C for 1 h, c) aged at 500 °C for 6 h and d) solution treated at 850 °C for 1 h and aged at 500 °C for 6 h.

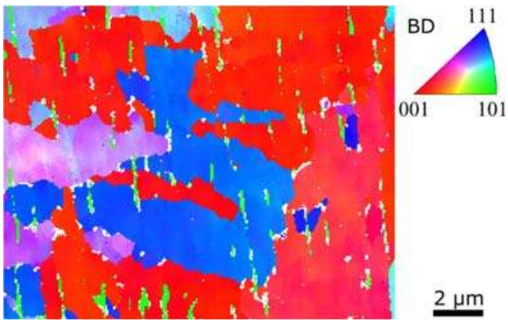

Figure 4. Orientation map obtained by EBSD for a 3D-printed sample aged at 500 °C for 6 h. The colour is based on the crystallographic orientation of the building direction (BD). The elongated features shown in green are austenite.

The microstructures of the as-printed and aged samples were investigated in further detail by TEM. As can be seen from figure 5, the as-printed sample has a dislocation structure with no visible evidence of precipitates. A few titanium oxides are observed, which are expected to originate from the printing process. After aging, precipitation is obvious (see figure 5b and c), and the dislocation structure observed in the printed condition is removed by the annealing. The larger elongated regions are found to be austenite, in agreement with the SEM EBSD results.

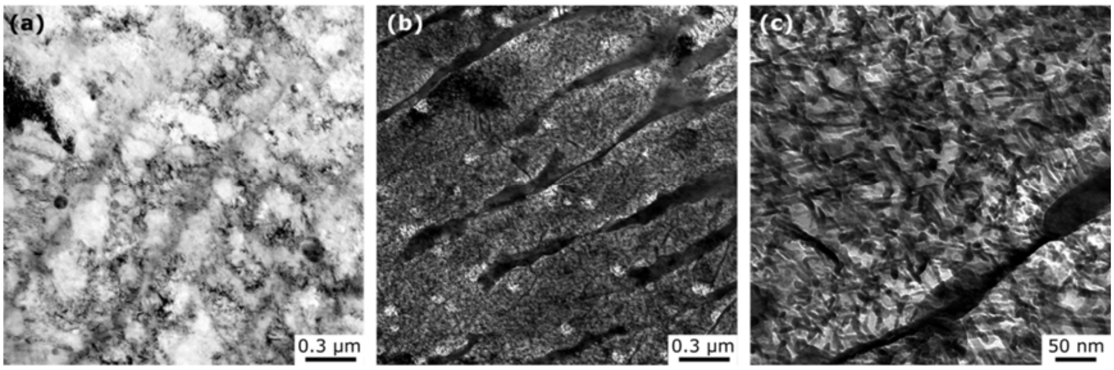

Figure 5. TEM micrographs of printed and aged samples. a) as-printed condition, b) aged at 500 °C for 6 h, c) higher magnification micrograph of the sample shown in b).

The microstructural observations reported above have significant effects on the mechanical properties. The Vickers hardness for all the printed, aged and solution treated samples as well as the conventional ones are reported in table 2. After solution treatment, the 3D-printed sample and the conventionally manufactured sample have a similar hardness. After aging, however, the hardness of the 3D-printed samples is lower than that of the conventional samples. It should be noted that the hardness measurements were carried out in zone 3 of the printed samples (see figure 1b), i.e. where the void density is very low. However, as demonstrated here, the voids still have a significant effect on the mechanical properties after aging although their effect is small in the solution treated condition.

Table 2. Averaged Vickers hardness values (the standard deviation is typically ~10).

	3D-printed	3D-printed solution treated	Conventional solution treated
Initial	377	324	329
480 °C 1/3/6 h	569/608/630	-/-/-	628/680/698
500 °C 1/3/6/10 h	598/615/633/600	621/637/642/-	649/679/688/-
520 °C 1/3/6/10 h	604/617/616/618	-/-/-	665/674/678/-

The aging treatment results in strengthening for all the samples. The highest hardness values of approximately 700 Vickers are obtained for the conventional sample. The aged 3D-printed samples have values in the range 600 – 640 Vickers, and the values after 10 h annealing at 540 °C and 520 °C indicate over-aging. The maximum hardness in this series of samples is observed after 6 h at 500 °C. Generally, it is reported in the literature that the additional solution treatment before aging of maraging steels leads to a reduction in yield strength and an improvement in elongation [2,6,9]. For the present 3D-printed samples, we do not observe any significant drop in hardness resulting from the additional solution treatment before aging. In fact, the solution treated sample aged at 500 °C for 6 h has the highest hardness among all the 3D-printed samples. This may be related to the fact that the printed and aged samples contain a significant fraction of soft austenite.

When relating the hardness results to the microstructural observations, it is clear that the precipitation that takes place during the aging treatment strengthens significantly the printed samples, as it does also for conventional processing. However, the peak aging condition appears to be at a slightly higher temperature (same annealing time) for the printed samples than for the conventional samples.

4. Summary

In the present work, aging of 3D-printed maraging steel samples has been compared to that of conventionally manufactured samples. It has been demonstrated that the 3D printing has a large effect on the microstructural evolution and on the hardness. Even the inner parts of the printed samples contain voids of sizes up to 15 μm, and although the fraction of voids is very low, it affects the hardness of the printed samples, especially in the aged condition. As in the conventionally manufactured samples, aging of the printed samples leads to precipitation and thus strengthening. However in printed and aged samples, a significant fraction of austenite is observed to be present, which may be avoided if the printed samples are solution treated before the aging. Depending on the application, the heat treatment of 3D-printed maraging steel components can be optimized, but the optimization parameters may be quite different from those for conventionally manufactured maraging steel.

Acknowledgement
DJJ, YBZ and TY thank the European Research Council (ERC) under the European Union's Horizon 2020 research and innovation programme (M4D – grant agreement No. 788567) for supporting part of this work.

References

[1] Becker T and Dimitrov D 2015 *Rapid Prototyping Journal*, **22** 487-494
[2] Kempen K, Yasa E, Thijs L, Kruth J P and Van Humbeeck J 2011 *Physics Procedia* **12** 255-263
[3] Mouritz A 2012 *Introduction to aerospace materials* (Cambridge: Woodhead Publishing Limited) p 244-246
[4] Guo W F, Guo C and Zhu Q 2018 *Materials Science Forum* **941** 2160-2166
[5] Lima Filho V X, Barros I F and Abreu H F 2017 *Materials Research* **20** 10-14
[6] Casati R, Lemke J N, Vedani M 2017 *La Metallurgia Italiana* **1** 11-20
[7] Bai Y, Yang Y, Wang D and Zhang M 2017 *Materials Science & Engineering A* **703** 116-123
[8] Mutua J, Nakata S, Onda T and Chen Z C 2018 *Materials & Design* **139** 486-497
[9] Tan C, Zhou K, Ma W, Zhang P, Liu M and Kuang T 2017 *Materials & Design* **134** 23-34